Structural Eng./Earthquake Eng., JSCE, Vol. 21, No. 2, 131s—142s, 2004 October
(J. Struct. Mech. Earthquake Eng., JSCE, No. 733/ I —69)

ANALYSIS OF CORRUGATED STEEL WEB GIRDERS BY AN EFFICIENT BEAM BENDING THEORY

Chawalit MACHIMDAMRONG[1], Eiichi WATANABE[2] and Tomoaki UTSUNOMIYA[3]

[1]Student member of JSCE, M. Eng., Graduate Student, Dept. of Civil and Earth Res. Eng., Kyoto University
(Yoshida-honmachi, Sakyo-ku, Kyoto 606-8501, Japan)
E-mail:chim@str.kuciv.kyoto-u.ac.jp
[2]Fellow of JSCE, Ph. D., Dr. Eng., Professor, Dept. of Civil and Earth Res. Eng., Kyoto University
(Yoshida-honmachi, Sakyo-ku, Kyoto 606-8501, Japan)
E-mail:watanabe@str.kuciv.kyoto-u.ac.jp
[3]Member of JSCE, Dr. Eng., Associate Professor, Dept. of Civil and Earth Res. Eng., Kyoto University
(Yoshida-honmachi, Sakyo-ku, Kyoto 606-8501, Japan)
E-mail:utsunomi@str.kuciv.kyoto-u.ac.jp

An elastic beam bending theory for analysis of prestressed concrete girders with corrugated steel web is derived by the application of the variational principle. The theory is a shear deformable beam theory which is based on three displacement fields and is similar to the classical Timoshenko beam theory. A two-node linear finite element with full and reduced integration of the theory is provided. It is then used to analyze simply supported and continuous I- and box-girders. Their predicted results are found in good agreement with those by the 3D finite element analysis. A simplified theory which is similar to the proposed theory by Kato *et al.* (2002) is also discussed and included in appendix.

Key Words: *shear deformable beam bending theory, corrugated steel web, variational principle, finite element analysis, reduced integration*

1. INTRODUCTION

Development of new material and innovation in construction technology always give birth to novel structures satisfying increasingly diversified demand: economy, durability and world-wide environmental requirements. Prestressed concrete girder with corrugated steel web, PCGCSW, is such a good example of the innovation that has been recently utilized in highway bridges. The PCGCSW has been considered superior to conventional girders in many aspects such as the reduction of the weight of superstructure and thus the cost of construction, easiness in maintenance, easiness in introduction of prestressing force and so forth.[1),2),3)]

However, such a new innovation must sometimes wait for the subsequent establishment of the basis. In the study of stress and deflection of the PCGCSW, the classical Euler-Bernoulli and Timoshenko beam theories were found not to be applicable as shear deformation in the corrugated steel web becomes large.[4)] Many researchers have worked on the deflection and stress analysis of the PCGCSW basing on numerical approaches[5),6)] and recently on the development of extended beam bending theories, e.g., the works of Kato *et al.*[7),8)], Machimdamrong *et al.*[4)] and a detailed theoretical study near an intermediate support by Shiratani *et al.*[9)]

In this study, an elastic shear deformable beam bending theory is derived. The theory is based on a set of assumed displacement fields: w, ψ, ϕ, as shown in **Fig. 1**. They are all in the sense of mean values.[10)] Separated rotational fields, ψ and ϕ account for shear deformation in the cross section and flanges of the girder. The theory thus seems to be a kind of the classical Timoshenko beam theory. Its equilibrium equations and boundary conditions are obtained by the principle of minimum potential energy, and a beam finite element is given with full and reduced integration.

Subsequently, the developed beam element is used to analyze a number of PCGCSWs, and their results are compared with those by the 3D finite element analysis and experimental data.

Similar but slightly different theories have been presented by the authors.[4] The sets of assumed displacement fields (w, α, ϕ) and ($\tilde{w}$, $\tilde{\alpha}$) are used in the theories (**Fig. 1** and **Fig. 18**). They are equally applicable to girders that possess longitudinal stiffness in the web; however, with *a priori* assumption on the neutral axis of the girders that is postulated to avoid difficulty in the theories, but raises unbalancing normal force in the cross section near points of abrupt change in shearing force. In contrast, the proposed theory developed herein satisfies perfectly the longitudinal equilibrium provided that in-plane compression-extension stiffness of the corrugated steel web is negligible.

2. AN ELASTIC SHEAR DEFORMABLE BEAM BENDING THEORY

In the derivation of the elastic shear deformable beam bending theory for analysis of the PCGCSW (referred to as G3-theory), a number of assumptions are made. They are stated below:

1. In-plane compression-extension stiffness of the corrugated steel web in the longitudinal direction is assumed to be negligible whereas shear stiffness in the web persists.
2. The assumption that plane section remains plane in the deformed state is discarded. Identical rotations in the x-z plane are assumed in the flanges, but are different from that of the cross section (**Fig. 1**: x-axis is along beam axis and z-axis points downward).
3. In-plane distortion of the cross section is prohibited.
4. Materials are within elastic range and their Poisson's ratios are assumed equivalently zero, except for calculation of shear modulus. Consequently, shear lag in the flanges is disregarded.
5. Transverse and prestressing forces are assumed to cause no twisting in the beam.
6. Transverse deflection of the beam is infinitesimal.

The first assumption is adopted from the fact that the corrugated steel plate utilized in the PCGCSW is considerably susceptible to shear deformation and possess negligible in-plane compression-extension stiffness (in a direction normal to its folded lines).[1),2)] In-plane bending deformation results from large geometrical change of the corrugation.

The second assumption is a consequence of the first one. The longitudinal displacement fields of the theory are defined based on the relative displacements of the upper and lower flanges which are characterized through a (mean) rotational fields, $\psi(x)$, connecting centroids of the flanges. Assumed identical rotations of the upper and lower flanges are taken into account by another rotational field, $\phi(x)$. The two displacement fields completely define warping of the cross section.

With the above consideration, shear deformations in the flanges and the web are equivalent to that in the classical Timoshenko beam theory (first-order shear deformable beam theory), and shear correction factors are usually required.[11),12)] However, a state of pure shear in the web is assumed in this study (shear correction factor = 1) according to the results of several bending experiments which show that measured longitudinal normal stress is almost zero except for localized areas adjacent to the flanges.[13),14)]

The remaining assumptions are those familiar in the classical beam bending theory.[15),16)]

The assumed displacement fields for the G3-theory are shown below (see **Fig. 1** and **Fig. 2**):

$$u^u(x,z) = r_1\psi(x) - (z+r_1)\phi(x), \tag{1}$$

$$u^w(x,z) = \{r_1 - \chi(z+l_1)\}\,\psi(x) - \left\{\frac{t_1}{2} - \rho(z+l_1)\right\}\phi(x), \tag{2}$$

$$u^l(x,z) = -r_2\psi(x) - (z-r_2)\phi(x), \tag{3}$$

$$w^u(x) = w^w(x) = w^l(x) = w(x), \tag{4}$$

here

$$\chi = \rho + 1,$$

$$\chi = \frac{r_1 + r_2}{l_1 + l_2}, \qquad \rho = \frac{t_1 + t_2}{2(l_1 + l_2)}.$$

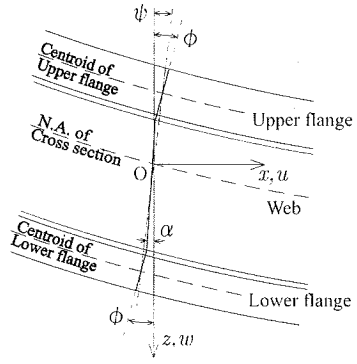

Fig. 1 Deformation of the PCGCSW according to the G3-theory.

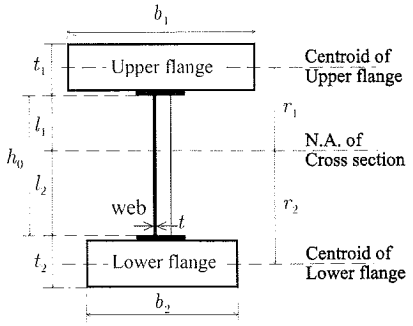

Fig. 2 Cross section of the PCGCSW.

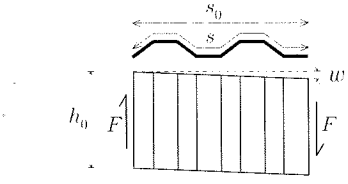

Fig. 3 Shear deformation of corrugated web.

Superscripts w, u and l refer to web, upper flange and lower flange, respectively. Geometric dimensions of a given section, l_1, l_2, etc. are shown schematically in **Fig. 2**. The web's longitudinal displacement function, u^w, is directly obtained by interpolation of the functions u^u and u^l at the interfaces of the flanges and the web. Note here that steel flanges are assumed to be properly transformed and included in the upper and lower concrete flanges. (Discussion on the relevant stiffnesses is given later)

The neutral axis of cross section as shown in **Fig. 2** is calculated by the first area moment equation considering only the upper and lower flanges. In this study, only rectangular section is considered for the flanges, though it is possible to extend to cover other shape as well (provided that the section is symmetry around vertical axis and a proper shear correction factor is applied).[10)]

The normal and average shear strains are derived based on the assumed displacement fields (normal strain in the web is disregarded according to the assumption 1):

$$\varepsilon^u_{xx} = r_1 \frac{\mathrm{d}\psi}{\mathrm{d}x} - (z + r_1)\frac{\mathrm{d}\phi}{\mathrm{d}x}, \tag{5}$$

$$\varepsilon^l_{xx} = -r_2 \frac{\mathrm{d}\psi}{\mathrm{d}x} - (z - r_2)\frac{\mathrm{d}\phi}{\mathrm{d}x}, \tag{6}$$

$$\gamma^u_{xz} = \frac{\mathrm{d}w}{\mathrm{d}x} - \phi, \tag{7}$$

$$\gamma^w_{xz} = \frac{\mathrm{d}w}{\mathrm{d}x} - \chi\psi + \rho\phi, \tag{8}$$

$$\gamma^l_{xz} = \frac{\mathrm{d}w}{\mathrm{d}x} - \phi. \tag{9}$$

The elastic extensional modulus of concrete flanges is denoted as E_1. The reduced elastic shear modulus of the web is denoted as G_0, and the elastic shear modulus of the flanges as G_1.

The reduced shear modulus of the web can be calculated from the following equation (see **Fig. 3**):

$$G_0 = \frac{s_0}{s} G. \tag{10}$$

Here, s_0 is the nominal longitudinal length, s is the actual longitudinal length and G is the elastic shear modulus of the corrugated steel plate. The equation was derived by considering equivalent shear deformation of the corrugated web.[17)]

The shear correction factor for the rectangular upper and lower flanges, κ, is supposed to be equal to $5/6$. For the web, however, the shear correction factor is not required. Consequently, the linear stress-strain relations can be written as follows (average in the case of shear stresses):

$$\sigma^u_{xx} = E_1 \varepsilon^u_{xx}, \qquad \tau^u_{xy} = \kappa G_1 \gamma^u_{xy}, \tag{11}$$

$$\sigma^l_{xx} = E_1 \varepsilon^l_{xx}, \qquad \tau^l_{xy} = \kappa G_1 \gamma^l_{xy}, \tag{12}$$

$$\tau^w_{xy} = G_0 \gamma^w_{xy}. \tag{13}$$

Therefore, the strain energy functional of the theory can be written as shown below (L is length of the beam):

$$U = \frac{1}{2}\int_0^L \left\{ \mathrm{g}_0 \left(\frac{\mathrm{d}w}{\mathrm{d}x} - \chi\psi + \rho\phi \right)^2 + \mathrm{g}_1 \left(\frac{\mathrm{d}w}{\mathrm{d}x} - \phi \right)^2 + \mathrm{e}_0 \left(\frac{\mathrm{d}\psi}{\mathrm{d}x} \right)^2 + \mathrm{e}_1 \left(\frac{\mathrm{d}\phi}{\mathrm{d}x} \right)^2 \right\} \mathrm{d}x, \tag{14}$$

where

$$\mathrm{e}_0 = E_1 \left(A_1 r_1^2 + A_2 r_2^2 \right),$$

$$\mathrm{e}_1 = E_1 \left(A_1 \frac{t_1^2}{12} + A_2 \frac{t_2^2}{12} \right),$$

$$\mathrm{g}_0 = G_0 A_0,$$

$$\mathrm{g}_1 = \mathrm{g}_1^u + \mathrm{g}_1^l,$$

$$\mathrm{g}_1^u = \kappa G_1 A_1, \quad \mathrm{g}_1^l = \kappa G_1 A_2.$$

Here, the sectional areas of the upper and lower flanges are $A_1 = b_1 t_1$ and $A_2 = b_2 t_2$. Sectional area of the web, A_0, is calculated by multiplying height of the web (h_0) by actual thickness of the web (t). The presence of the steel flanges in the girder is taken into the above stiffness constants by considering that e_0 is

the product of modulus and the second area moment of the upper and lower flanges considering them as point masses. Also, $\mathbf{e}_1$ is the product of the modulus and the second area moment of the upper and lower flanges around their centroids.

The first and second terms in the strain energy functional represent the first-order shear deformation energy in the web and flanges, respectively.

Next, the external potential energy functional of the transverse load, $\bar{q}$, is:

$$V = -\int_0^L \bar{q} w \, \mathrm{d}x, \tag{15}$$

and the total potential energy functional is:

$$\Pi = U + V. \tag{16}$$

The equilibrium equations and the boundary conditions of the G3-theory can be obtained by the principle of minimum potential energy, which has a statement as shown below:[15]

$$\delta\Pi = \frac{\partial \Pi}{\partial w}\delta w + \frac{\partial \Pi}{\partial \psi}\delta\psi + \frac{\partial \Pi}{\partial \phi}\delta\phi = 0. \tag{17}$$

Calculating the above variation, integrating by part of the functional and invoking arbitrariness of each variation, the following equilibrium equations and boundary conditions are obtained:

Equilibrium equations corresponding to δw, $\delta\psi$ and $\delta\phi$, respectively:

$$\bar{q} = -\mathbf{g}_0\left(\frac{\mathrm{d}^2 w}{\mathrm{d}x^2} - \chi\frac{\mathrm{d}\psi}{\mathrm{d}x} + \rho\frac{\mathrm{d}\phi}{\mathrm{d}x}\right) - \mathbf{g}_1\left(\frac{\mathrm{d}^2 w}{\mathrm{d}x^2} - \frac{\mathrm{d}\phi}{\mathrm{d}x}\right), \tag{18}$$

$$0 = \chi\mathbf{g}_0\left(\frac{\mathrm{d}w}{\mathrm{d}x} - \chi\psi + \rho\phi\right) + \mathbf{e}_0\frac{\mathrm{d}^2\psi}{\mathrm{d}x^2}, \tag{19}$$

$$0 = \rho\mathbf{g}_0\left(\frac{\mathrm{d}w}{\mathrm{d}x} - \chi\psi + \rho\phi\right) - \mathbf{g}_1\left(\frac{\mathrm{d}w}{\mathrm{d}x} - \phi\right) - \mathbf{e}_1\frac{\mathrm{d}^2\phi}{\mathrm{d}x^2}, \tag{20}$$

and *Boundary conditions* prescribing ones of the following:

$$w \quad \text{or} \quad \mathbf{g}_0\left(\frac{\mathrm{d}w}{\mathrm{d}x} - \chi\psi + \rho\phi\right) + \mathbf{g}_1^u\left(\frac{\mathrm{d}w}{\mathrm{d}x} - \phi\right) + \mathbf{g}_1^l\left(\frac{\mathrm{d}w}{\mathrm{d}x} - \phi\right), \tag{21}$$

$$\psi \quad \text{or} \quad -\mathbf{e}_0\frac{\mathrm{d}\psi}{\mathrm{d}x}, \tag{22}$$

$$\phi \quad \text{or} \quad -\mathbf{e}_1\frac{\mathrm{d}\phi}{\mathrm{d}x}. \tag{23}$$

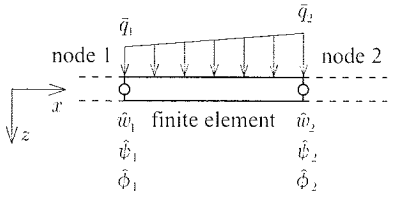

Fig. 4 Two-node linear finite element.

The first term in the vertical displacement boundary condition (Eq. 21) is shearing force in the web, while the second and third terms are shearing force in the upper and lower flanges, respectively. Their summation is the shearing force acting on the cross section of the beam. The second boundary condition (Eq. 22) represents the only bending moment acting on the section when the cross section rotates without any rotation in the flanges. The rotations of the upper and lower flanges induce additional bending moment on the section as implied in the third boundary condition. Their summation is the bending moment acting on cross section of the beam.

The equilibrium equations (Eqs. 18 to 20) and boundary conditions (Eqs. 21 to 23) constitute a system of differential equations for beam bending problem.

Note here that the expressions for force-resultant can be readily derived by integrating the stress-strain relations (Eqs. 11 to 13).

3. FINITE ELEMENT FORMULATION

The displacement fields in the G3-theory are numerically approximated in the finite element analysis by interpolation of nodal displacement unknowns with appropriate shape functions (**N**'s). In general, these can be written as shown below:

$$w \approx \mathbf{N}_w^T\hat{\mathbf{w}}, \quad \psi \approx \mathbf{N}_\psi^T\hat{\boldsymbol{\psi}}, \quad \phi \approx \mathbf{N}_\phi^T\hat{\boldsymbol{\phi}}. \tag{24}$$

The system equation in relation to the stiffness matrix (**K**), nodal displacement unknown vector ($\boldsymbol{\theta}$) and external forces vector (**f**) can be written as follows:

$$\mathbf{K}\boldsymbol{\theta} = \mathbf{f}, \tag{25}$$

where

$$\mathbf{K} = \begin{bmatrix} \mathbf{K}_{11} & \mathbf{K}_{12} & \mathbf{K}_{13} \\ \vdots & \mathbf{K}_{22} & \mathbf{K}_{23} \\ \text{Sym.} & \cdots & \mathbf{K}_{33} \end{bmatrix},$$

$$\boldsymbol{\theta} = \begin{Bmatrix} \hat{\mathbf{w}} \\ \hat{\boldsymbol{\psi}} \\ \hat{\boldsymbol{\phi}} \end{Bmatrix}, \qquad \mathbf{f} = \begin{Bmatrix} \mathbf{f}_1 \\ 0 \\ 0 \end{Bmatrix}.$$

The stiffness matrix is symmetric because the strain energy functional is positive definite.[18] Substituting the assumed displacement fields (Eq. 24) into the total potential energy functional, one can explicitly write the elements of the stiffness matrix:

$$\mathbf{K}_{11} = (\mathbf{g}_0 + \mathbf{g}_1) \int_0^L \frac{\mathrm{d}\mathbf{N}_w}{\mathrm{d}x} \frac{\mathrm{d}\mathbf{N}_w^T}{\mathrm{d}x} \mathrm{d}x, \tag{26}$$

$$\mathbf{K}_{12} = \mathbf{K}_{21}^T = -\chi \mathbf{g}_0 \int_0^L \frac{\mathrm{d}\mathbf{N}_w}{\mathrm{d}x} \mathbf{N}_\psi^T \mathrm{d}x, \tag{27}$$

$$\mathbf{K}_{13} = \mathbf{K}_{31}^T = (\rho \mathbf{g}_0 - \mathbf{g}_1) \int_0^L \frac{\mathrm{d}\mathbf{N}_w}{\mathrm{d}x} \mathbf{N}_\phi^T \mathrm{d}x, \tag{28}$$

$$\mathbf{K}_{22} = \mathbf{e}_0 \int_0^L \frac{\mathrm{d}\mathbf{N}_\psi}{\mathrm{d}x} \frac{\mathrm{d}\mathbf{N}_\psi^T}{\mathrm{d}x} \mathrm{d}x + \chi^2 \mathbf{g}_0 \int_0^L \mathbf{N}_\psi \mathbf{N}_\psi^T \mathrm{d}x, \tag{29}$$

$$\mathbf{K}_{23} = \mathbf{K}_{32}^T = -\rho\chi \mathbf{g}_0 \int_0^L \mathbf{N}_\psi \mathbf{N}_\phi^T \mathrm{d}x, \tag{30}$$

$$\mathbf{K}_{33} = \mathbf{e}_1 \int_0^L \frac{\mathrm{d}\mathbf{N}_\phi}{\mathrm{d}x} \frac{\mathrm{d}\mathbf{N}_\phi^T}{\mathrm{d}x} \mathrm{d}x + (\rho^2 \mathbf{g}_0 + \mathbf{g}_1) \int_0^L \mathbf{N}_\phi \mathbf{N}_\phi^T \mathrm{d}x, \tag{31}$$

$$\mathbf{f}_1 = \int_0^L \mathbf{N}_w \bar{q} dx. \tag{32}$$

Here, a two-node six-degree of freedom linear element is considered in applying the above formulation because of its practicability and easiness in coding. Note that no distinction is made between element quantities and system quantities as they are actually the same concept.

The element stiffness matrix and the external force vector are derived by assuming linear interpolation (see **Fig. 4**) in every shape function:

$$\mathbf{N}_w^T = \mathbf{N}_\psi^T = \mathbf{N}_\phi^T = \mathbf{N}^T = \left[\, 1 - \frac{x}{L} \quad \frac{x}{L} \,\right], \tag{33}$$

with the corresponding nodal displacement unknown vector:

$$\boldsymbol{\theta}^T = [\, \hat{w}_1 \quad \hat{\psi}_1 \quad \hat{\phi}_1 \quad \hat{w}_2 \quad \hat{\psi}_2 \quad \hat{\phi}_2 \,]. \tag{34}$$

Additionally, the vertical loading, $\bar{q}$, is interpolated by the same linear shape function:

$$\bar{q} = \left[\, 1 - \frac{x}{L} \quad \frac{x}{L} \,\right] \left\{ \begin{array}{c} \bar{q}_1 \\ \bar{q}_2 \end{array} \right\} = \mathbf{N}^T \bar{\mathbf{q}}. \tag{35}$$

Substituting the nodal displacement unknown vector and the above vertical loading into Eqs. 26 to 32, the following stiffness matrix (which is decomposed into those from bending terms and shear terms, $\mathbf{K} = \mathbf{K}_b + \mathbf{K}_s$) and force vector, $\mathbf{f}_1$, are obtained:

$$\mathbf{K}_b = \frac{1}{L} \begin{bmatrix} 0 & 0 & 0 & 0 & 0 & 0 \\ & \mathbf{e}_0 & 0 & 0 & -\mathbf{e}_0 & 0 \\ & & \mathbf{e}_1 & 0 & 0 & -\mathbf{e}_1 \\ & & & 0 & 0 & 0 \\ & \text{Sym.} & & & \mathbf{e}_0 & 0 \\ & & & & & \mathbf{e}_1 \end{bmatrix}, \tag{36}$$

$$\mathbf{K}_s = \frac{1}{6L} \begin{bmatrix} 6(\mathbf{g}_0+\mathbf{g}_1) & 3\chi\mathbf{g}_0 L & -3(\rho\mathbf{g}_0-\mathbf{g}_1)L & -6(\mathbf{g}_0+\mathbf{g}_1) & 3\chi\mathbf{g}_0 L & -3(\rho\mathbf{g}_0-\mathbf{g}_1)L \\ & 2\chi^2\mathbf{g}_0 L^2 & -2\rho\chi\mathbf{g}_0 L^2 & -3\chi\mathbf{g}_0 L & \chi^2\mathbf{g}_0 L^2 & -\rho\chi\mathbf{g}_0 L^2 \\ & & 2(\rho^2\mathbf{g}_0+\mathbf{g}_1)L^2 & 3(\rho\mathbf{g}_0-\mathbf{g}_1)L & -\rho\chi\mathbf{g}_0 L^2 & (\rho^2\mathbf{g}_0+\mathbf{g}_1)L^2 \\ & \text{Sym.} & & 6(\mathbf{g}_0+\mathbf{g}_1) & -3\chi\mathbf{g}_0 L & 3(\rho\mathbf{g}_0-\mathbf{g}_1)L \\ & & & & 2\chi^2\mathbf{g}_0 L^2 & -2\rho\chi\mathbf{g}_0 L^2 \\ & & & & & 2(\rho^2\mathbf{g}_0+\mathbf{g}_1)L^2 \end{bmatrix}, \tag{37}$$

$$\mathbf{f}_1 = \left\{ \begin{array}{c} f_1 \\ f_4 \end{array} \right\} = \frac{L}{6} \begin{bmatrix} 2 & 1 \\ 1 & 2 \end{bmatrix} \left\{ \begin{array}{c} \bar{q}_1 \\ \bar{q}_2 \end{array} \right\}. \tag{38}$$

The finite element developed here is referred to as *G3F element*.

4. REDUCED INTEGRATION

The stiffness matrixes for bending and shear terms as shown in Eqs. 36 and 37 are exact, or in other word, fully integrated. The full integration on shear term in a similar element as the Timoshenko beam element may incur *shear locking*.[18] The G3F element also suffers from the phenomenon. The locking can be avoided by either using lower order interpolation or simply recourse to reduced integration in shear terms.[19),20]

The reduced integration scheme is chosen here because of its simplicity. Consequently, the fully integrated shear stiffness matrix ($\mathbf{K}_s$) must be modified. This can be done by replacing some constants in the matrix as follows (Symmetry must be preserved):

$$\mathbf{K}_{s_{22}} = \mathbf{K}_{s_{25}} = \mathbf{K}_{s_{55}} = \frac{3}{2}\chi^2 \mathbf{g}_0 L^2,$$

$$\mathbf{K}_{s_{23}} = \mathbf{K}_{s_{26}} = \mathbf{K}_{s_{35}} = \mathbf{K}_{s_{56}} = -\frac{3}{2}\rho\chi \mathbf{g}_0 L^2,$$

$$\mathbf{K}_{s_{33}} = \mathbf{K}_{s_{36}} = \mathbf{K}_{s_{66}} = \frac{3}{2}(\rho^2 \mathbf{g}_0 + \mathbf{g}_1) L^2.$$

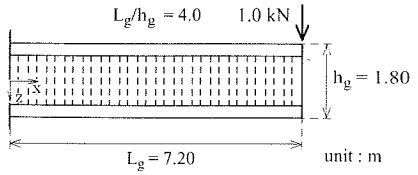

Fig. 5 I-section cantilever subjected to tip load.

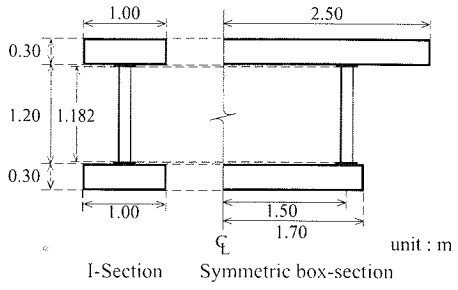

Fig. 6 I- and box-sections.

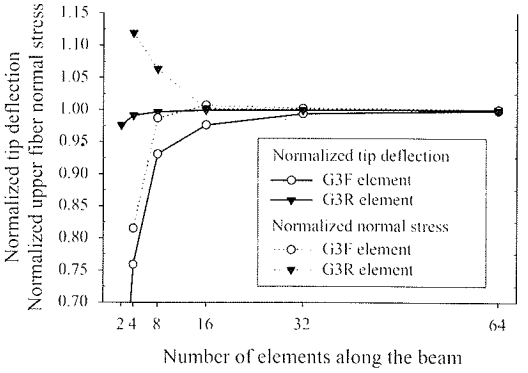

Fig. 7 Convergence of G3F and G3R elements.

This reduced integration element is referred to as *G3R element*. The performance of the G3F and G3R elements is examined by considering an I-section cantilever subjected to a vertical end load as shown in **Fig. 5**. The cross section of the I-cantilever is shown in **Fig. 6**. The plane remains plane condition is assumed at its free end. Material constants and sectional details are the same as those assumed in the next section and they are deferred to be discussed there.

Calculated tip deflection of the cantilever is normalized with the exact solution (see theories and solutions given in reference 4, which are equivalent to the present one in the case of I-section) and plotted in **Fig. 7** with respect to the number of elements along the cantilever (uniform division). In the same figure, interpolated upper fiber normal stress in the upper flange at x = 0.90 m is also shown. It is obvious that the G3R element exhibits better performance to the G3F element for deflection prediction. For stress prediction, the G3F element seems to yield better convergence, however, this is not conclusive because both elements were derived based on displacement interpolation.

For the I-section cantilever, a uniform division to the elements of ratio L/h_g = 1/512 is still error-free on general Intel-based computer. It is thought that the element is robust enough for general application.

5. NUMERICAL EXAMPLES

(1) Simply supported I- and box-section PCGCSWs

In this section, a number of PCGCSWs are analyzed by utilizing the G3R element. Its prediction are compared with those modeled and analyzed by a commercial finite element program, ABAQUS. Note here that the PCGCSWs analyzed here are the same as in the reference 4.

The PCGCSWs are different in their sectional geometry, magnitudes of prestressing and loading, while their longitudinal configurations are the same as shown in **Fig. 8**. I- and Box-sections are considered in this study (**Fig. 6**). The corrugated steel web is stiffened with 9-mm thick, 25-cm width stiffeners at points A–G, and the upper and lower steel flange of the same sectional dimension. The girders are simply supported and are loaded with two different load cases, 4-point load and distributed load.

Material properties are shown in **Table 1**, and additionally, the ultimate strength of concrete is assumed to be 40 MN/m^2. For brevity, only long term loading condition is considered in this analysis. Therefore, the effective prestressing force is of concern, and is supposed to create approximately 40% of the concrete's ultimate strength at lower fiber and zero at upper fiber of the girder at mid span. The magnitude of load on each girder for each load case is then calculated to neutralize the lower fiber stress at mid span. The prestressing forces and transverse loads are summarized in **Table 2**.

(2) 3D finite element analysis using ABAQUS

The three dimensional finite element analysis is also carried out in the ABAQUS.[21] The concrete flanges are built up from the 3D eight-node linear brick element, C3D8. The corrugated steel web, steel flanges and stiffeners are assembled from the four-node linear shell element, S4. Specifically, a strip of the corrugated steel web is composed of 4×12 S4 elements with parabolically varying aspect ratios from

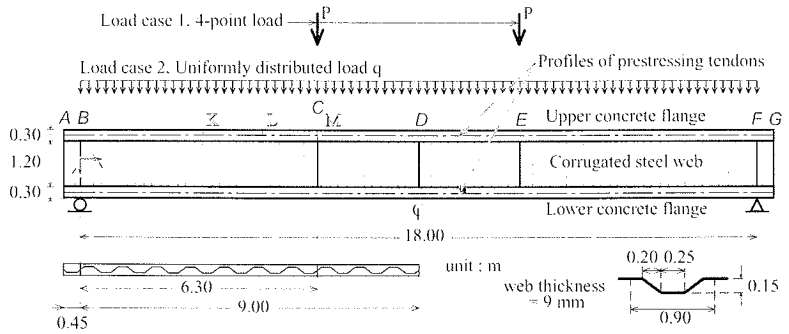

Fig. 8 Simply supported girder under load case 1 and case 2, and its details.

Table 1 Materials' properties.

Modulus	Value [GN/m^2]
Web's reduced shear modulus, G_0	69.23
Flanges' extensional modulus, E_1	31.00
Flanges' shear modulus, G_1	12.92

Table 2 Prestressing forces and loads.

Forces	Section	
	I	Box
Prestressing force, upper flange [MN]	0.315	1.80
Prestressing force, lower flange [MN]	4.50	15.30
4–point load, P (case 1) [MN]	1.00	3.40
Distributed load, q (case 2) [MN/m]	0.16	0.54

Table 3 Convergence of the G3R element.

No. of element	5	10	20	40
Normalized deflection (%)	97.6	99.4	99.9	100.0

1.24 to 2.00 (uniform in horizontal direction but concentrated at the upper and lower portions). The number of S4 elements employed is 4,320 in both sections, and those of the C3D8 elements are 21,504 and 29,568 in the I- and Box-sections, respectively. Rigid elements are used to impose the condition of plane section remains plane at the prestressing end as well as restraining relative longitudinal displacement in the flanges to prevent shear lag.

Fig. 9 shows the magnified deformation of the box-girder under 4-point loading.

(3) Analysis by the G3R element

For the analysis by the G3R element, the girders are modeled only for the left half because of their symmetry. The condition on plane section remains plane at the left end is achieved by assigning the same degree of freedom for the rotations $\hat{\psi}$ and $\hat{\phi}$. Vertical deflection ($\hat{w}$) is fixed at left support, while the rotations $\hat{\psi}$ and $\hat{\phi}$ are also fixed at mid span.

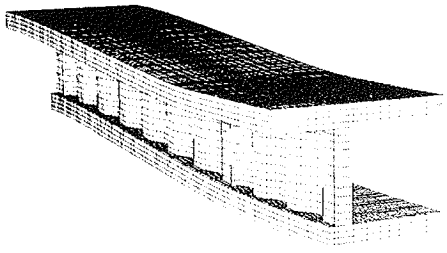

Fig. 9 Magnified deformation of a quarter of box-girder under 4-point loading.

Prestressing moment is applied directly at their left end while prestressing normal stress is calculated separately by the superposition principle.

(4) Results and discussions

a) Convergence

Convergence of the solution by the G3R element is firstly checked by comparing midspan deflection of the I-girder under uniformly distributed load with various mesh refinements. An incremental uniform refinement is done between midspan and left support while holding two elements toward prestressing end. The convergence is found to be very fast as shown in **Table 3**, and 40-element uniform mesh is utilized in this analysis (42 elements in total).

b) Vertical deflection

Deflection of the I-girder under distributed loading and the box-girder under 4-point loading are shown in **Fig. 10** and **Fig. 11**. Note that some results are not shown here because of their similarity. In the figures, *ABAQUS* refers to the results by the ABAQUS program. Additionally, *ABAQUS w/o Shear lag* refers to the results by the ABAQUS for the case that shear lag in the flanges is prevented. The shear lag in flange is not considered in this study and is thought that the phenomenon can be studied by utilizing the effective width concept. Also shown in the figures are the predictions by the theory proposed by Kato *et al.*[7),8)]

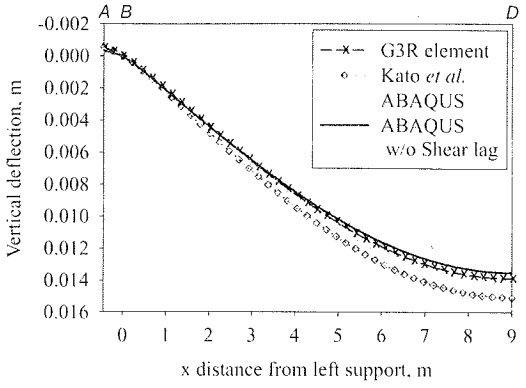

Fig. 10 Vertical deflection of I-girder under distributed loading.

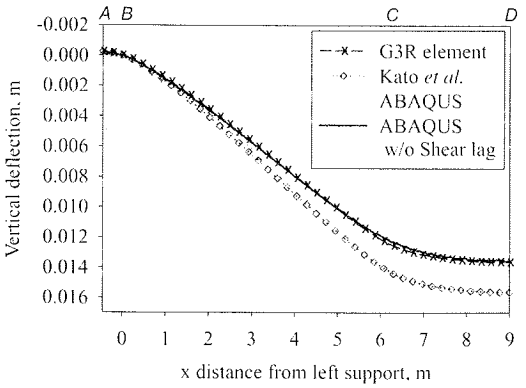

Fig. 11 Vertical deflection of box-girder under 4-point loading.

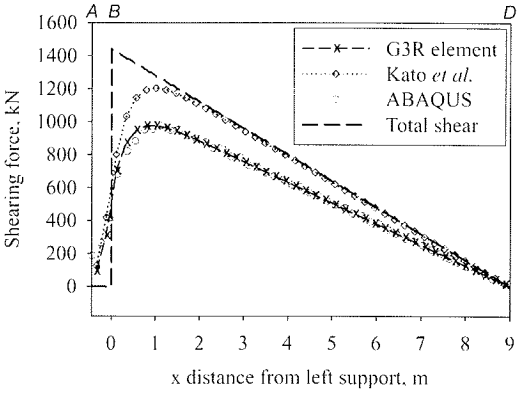

Fig. 12 Shearing force in web of I-girder under distributed loading.

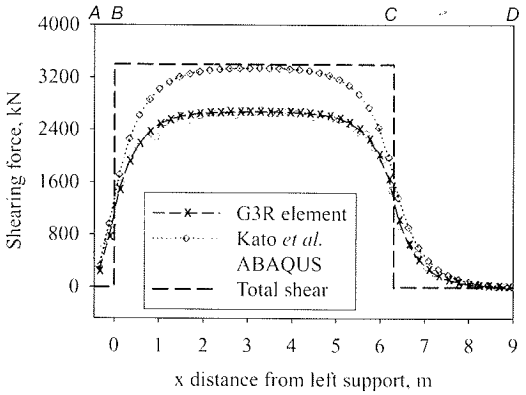

Fig. 13 Shearing force in web of box-girder under 4-point loading.

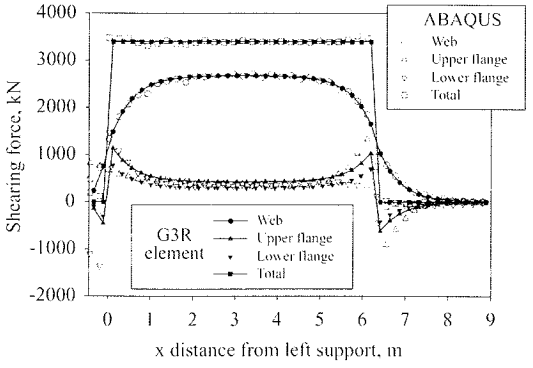

Fig. 14 Shearing forces in box-girder under 4-point loading.

It is clear from the figures that the deflections predicted by the G3R element are very close to those by ABAQUS, especially in the case that shear lag in the flanges is prohibited while the theory proposed by Kato *et al.* seems to overestimate the deflection.

c) Shearing forces

Fig. 12 and **Fig. 13** show shearing force in the corrugated steel web for the I-girder under distributed loading and the box-girder under 4-point loading. Clearly, the G3R element predicts the shearing forces in good agreement with those by the ABAQUS, both for 4-point loading and distributed loading. Exaggerating in shearing force predicted by the theory of Kato *et al.* is also observed.

Shearing forces in flanges and web of the box-girder are closely investigated for the case of 4-point loading. They are plotted in **Fig. 14**. Note here that shearing force in the steel flanges calculated by ABAQUS is not included in the plot. Their magnitude constitutes only a small fraction in this analysis.

In general, the shearing forces predicted by the G3R element are very close to those by ABAQUS. However, there is some discrepancy at the points of abrupt change of shearing force. At the support (x =

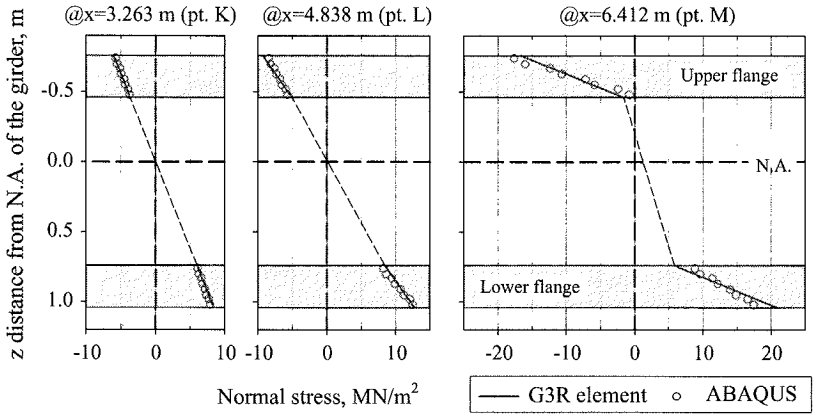

Fig. 15 Normal stresses at points K, L and M in the upper and lower flanges of box-girder under 4-point loading.

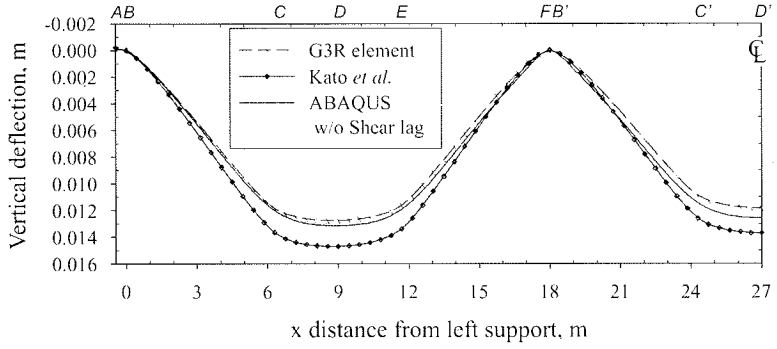

Fig. 16 Deflection of 3-span continuous box-girder under load case 1 (Points C, E, C':Loading points; B, B':Supports; D':Center of girder)

0 m), the G3R element underestimates the change of shearing force in the lower flange, but overestimates at the point of applying loading (x = 6.3 m). On the other hand, it is reversed in the upper flange. This shows a fact that stress concentration is unavoidable in actual structure and does not reveal itself in the beam theory. Nevertheless, the G3R element is found acceptably accurate to an extent.

d) Normal stresses in flanges

For the same box-girder under 4-point loading, calculated normal stresses in the upper and lower flanges at points K, L and M are shown in **Fig. 15** (see **Fig. 8**). Only the stresses induced by transverse loading are plotted here. The G3R element yields a very close prediction at every point as shown in the figure even at a point near abrupt change of shearing force (pt. M).

(5) Three-span continuous box-girder

To further show the application of the G3R element, a three-span continuous box girder is analyzed. The girder's section is supposed to be the same as shown in **Fig. 6**, and it is assumed to be an extension of the girder in **Fig. 8**, by duplicating 18 m segment B–F, three times to its right, and labelling them as B'–F' and B''–F''. Its total length is 0.45+18.0+18.0+18.0+0.45 = 54.9 m. The girder is loaded in the same manner with the box girder under 4-point loading analyzed previously; Point loads at C, E, C', E', C'' and E''. Prestressing force is also supposed to be the same as that for the box section as shown in **Table 2**.

Fig. 16 shows the calculated vertical deflection of the girder. From the figure, the G3R element seems to slightly underestimate its vertical deflection compared to the result of the finite element analysis. By considering the result of the finite element analysis, large increment in the vertical deflection is observed at the localized areas of the girder's supports. Higher order shear deformation in the flanges and large geometric change in the corrugated steel web (thus further decrement of shear modulus) are anticipated at

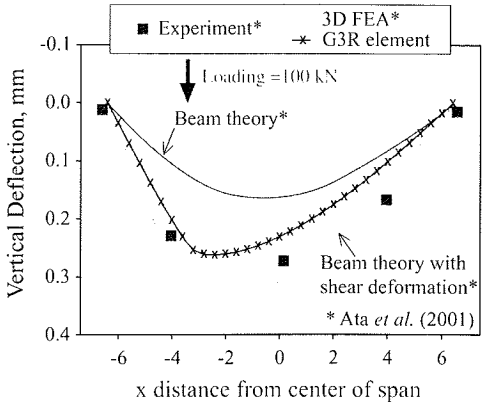

Fig. 17 Deflection of I-girder in step 5, Ata *et al.*[22]

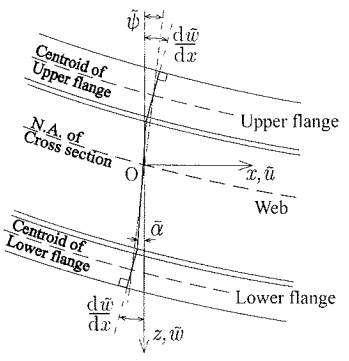

Fig. 18 Sectional deformation of PCGCSW according to the G2-theory.

these points. Beside that, the support condition is difficult to be modeled in the finite element analysis. The above factors are thought to contribute to the difference.

(6) Comparison with experimental data

The G3R element is applied to analyze a simply supported I-girder under 4-point load in the experiment by Ata *et al.*[22] The deflections of the I-girder at step 5 are shown in **Fig. 17**. The prediction by G3R element is close to the 3D finite element analysis by Ata *et al.*, but they are slightly different from the experimental data. However, according to Ata *et al.*, discontinuous connections of the steel flanges and slip between the flanges and concrete were not considered in their numerical analysis , and are regarded as the main contribution of the difference.

Shear strain in the corrugated web at mid span of the girder is predicted by the G3R element to be approximately about 15.4×10^{-6} . It is also in agreement with the results by the 3D finite element analysis by Ata *et al.* which is close to the experimental data.

6. CONCLUSIONS

An elastic beam bending theory (G3-theory) and its finite element implementation have been proposed for deflection and stress analysis of corrugated steel web girder.

Numerical examples on I- and box-section girders utilizing the developed element (G3R element) showed good correlations with the results calculated by the 3D finite element analysis. This validates the derived theory and shows the accuracy of the developed finite element.

Additionally, the theory was found to be applicable for studying of the shear lag phenomenon in the corrugated steel web, which is important for bridge designers.

In conclusion, it is suggested that the beam bending theory and its finite element developed in this study can be applied for deflection and stress analysis of the PCGCSW.

APPENDIX A SIMPLIFIED THEORY

The developed G3-theory can be simplified into a theory which is based on two unknown displacement fields (referred to as G2-theory).

The two fields are the vertical deflection of the beam ($\tilde{w}$) and the rotation of cross section ($\tilde{\psi}$). The rotations of both flanges are assumed to be equal to the first derivative of its vertical deflection (as shown in **Fig. 18**). The theory seems similar to a combination of the classical Euler-Bernoulli and Timoshenko beam theories. Note that the same assumption was also used in the theory by Kato *et al.*[7]

The assumed displacement fields are given as follows:

$$\tilde{u}^u(x,z) = r_1\tilde{\psi}(x) - (z+r_1)\frac{\mathrm{d}\tilde{w}(x)}{\mathrm{d}x}, \tag{39}$$

$$\tilde{u}^w(x,z) = \{r_1 - \chi(z+l_1)\}\,\tilde{\psi}(x) - \left\{\frac{t_1}{2} - \rho(z+l_1)\right\}\frac{\mathrm{d}\tilde{w}(x)}{\mathrm{d}x}, \tag{40}$$

$$\tilde{u}^l(x,z) = -r_2\tilde{\psi}(x) - (z-r_2)\frac{\mathrm{d}\tilde{w}(x)}{\mathrm{d}x}, \tag{41}$$

$$\tilde{w}^u(x) = \tilde{w}^w(x) = \tilde{w}^l(x) = \tilde{w}(x). \tag{42}$$

The strain energy functional of the theory is as

shown below:

$$\tilde{U} = \frac{1}{2}\int_0^L \left\{ \chi^2 \mathbf{g}_0 \left(\frac{\mathrm{d}\tilde{w}}{\mathrm{d}x} - \tilde{\psi} \right)^2 + \mathbf{e}_0 \left(\frac{\mathrm{d}\tilde{\psi}}{\mathrm{d}x} \right)^2 + \mathbf{e}_1 \left(\frac{\mathrm{d}^2\tilde{w}}{\mathrm{d}x^2} \right)^2 \right\} \mathrm{d}x. \tag{43}$$

The external potential energy functional and the total potential energy functional are similar to Eqs. 15 and 16. By carrying out the same procedure discussed in Section 2, one can obtain:

Equilibrium equations corresponding to $\delta\tilde{w}$ and $\delta\tilde{\psi}$, respectively:

$$\bar{q} = -\chi^2 \mathbf{g}_0 \left(\frac{\mathrm{d}^2\tilde{w}}{\mathrm{d}x^2} - \frac{\mathrm{d}\tilde{\psi}}{\mathrm{d}x} \right) + \mathbf{e}_1 \frac{\mathrm{d}^4\tilde{w}}{\mathrm{d}x^4}, \tag{44}$$

$$0 = \chi^2 \mathbf{g}_0 \left(\frac{\mathrm{d}\tilde{w}}{\mathrm{d}x} - \tilde{\psi} \right) + \mathbf{e}_0 \frac{\mathrm{d}^2\tilde{\psi}}{\mathrm{d}x^2}, \tag{45}$$

and *Boundary conditions*:

$$\tilde{w} \quad \text{or} \quad \chi^2 \mathbf{g}_0 \left(\frac{\mathrm{d}\tilde{w}}{\mathrm{d}x} - \tilde{\psi} \right) - \mathbf{e}_1 \frac{\mathrm{d}^3\tilde{w}}{\mathrm{d}x^3}, \tag{46}$$

$$\tilde{\psi} \quad \text{or} \quad -\mathbf{e}_0 \frac{\mathrm{d}\tilde{\psi}}{\mathrm{d}x}, \tag{47}$$

$$\frac{\mathrm{d}\tilde{w}}{\mathrm{d}x} \quad \text{or} \quad -\mathbf{e}_1 \frac{\mathrm{d}^2\tilde{w}}{\mathrm{d}x^2}. \tag{48}$$

Among the theory's stress-resultant relations, it is interesting to discuss shearing forces in the web and the flanges. They are as shown below:

$$\tilde{Q}^w = \chi \mathbf{g}_0 \left(\frac{\mathrm{d}\tilde{w}}{\mathrm{d}x} - \tilde{\psi} \right), \tag{49}$$

$$\tilde{Q}^u + \tilde{Q}^l = \rho\chi \mathbf{g}_0 \left(\frac{\mathrm{d}\tilde{w}}{\mathrm{d}x} - \tilde{\psi} \right) - \mathbf{e}_1 \frac{\mathrm{d}^3\tilde{w}}{\mathrm{d}x^3}. \tag{50}$$

Shearing force in the web can be obtained directly by integration of web's shear strain. But those of the flanges must be considered from equilibrium condition. As can be seen in Eq. 50, they are augmented by web-shear deformation related term (the first term) because of their assumed displacement fields that involve with both $\tilde{w}$ and $\tilde{\psi}$. Here, the familiar vertical load-deformation equation of the classical Euler-Bernoulli beam theory (i.e., $Q = -\mathbf{e}_1 \frac{\mathrm{d}^3 w}{\mathrm{d}x^3}$) is not intuitively applied.

The amount of additional shearing force depends on parameters ρ and χ, which relate directly to the depth of the girder and thickness of the flanges. In general, as the girder becomes deeper and the flanges become thinner, the smaller shearing force in the flanges.

The beam bending theory proposed by Kato *et al.*[7),8)] was derived based on the equilibrium of cross section. The procedure gave the strain energy functional similar to Eq. 43, but with χ instead of χ^2. This exaggerates shearing force in the web and overestimates the deflection.

REFERENCES

1) Combault, J.: The Maupre viaduct near Charolles, France, *J. Japan Prest. Conc. Eng. Assoc.*, Vol. 34, No. 1, pp. 63–71, 1992. (in Japanese, Ohura, T.: translator)
2) Johnson, R. P. and Cafolla, J.: Corrugated webs in plate girders for bridges, *Proc. Inst. Civ. Eng., Struct. Build.*, Vol. 123, May, pp. 157–164, 1997.
3) Watanabe, E., Kadotani, T., Kano, M., Utsunomiya, T. and Machimdamrong, C.: Corrugated steel webs in prestressed girders, *Proc. 4th U.S.-Japan Seminar on Advanced Stability and Seismicity Concept for Performance-based Design of Steel and Composite Structures, Japan, Kyoto, July 23–26*, 2001.
4) Machimdamrong, C., Watanabe, E. and Utsunomiya, T.: An extended elastic shear deformable beam theory and its application to corrugated steel web girder, *J. Struct. Eng.*, JSCE, Vol. 49A, pp. 29–38, 2003.
5) Taniguchi, N. and Yoda, T.: Study on a simple method for bending analysis of composite girders with corrugated steel webs, *J. Struct. Mech. Earthquake Eng.*, JSCE, No. 577(I-41), pp. 107–120, 1997. (in Japanese)
6) Shirozu, A., Sano, Y. and Oshita, S.: A study of analytical method using "the constant shear flow panels" for composite bridges with corrugated steel webs, *J. Struct. Eng.*, JSCE, Vol. 46A, pp. 1667–1674, 2000. (in Japanese)
7) Kato, H., Kawabata, A. and Nishimura, N.: Practical calculation formula on displacements and stress resultants of steel-concrete mixed girders with corrugated steel web, *J. Struct. Mech. Earthquake Eng.*, JSCE, No. 703(I-59), pp. 293–300, 2002. (in Japanese)
8) Kato, H. and Nishimura, N.: Practical analysis of continuous girders and cable stayed bridges with corrugated steel web, *J. Struct. Mech. Earthquake Eng.*, JSCE, No. 731(I-63), pp. 231–245, 2003. (in Japanese)
9) Shiratani, H., Ikeda, H., Imai, Y. and Kano, K.: Flexural and shear behavior of composite bridge girder with corrugated steel webs around middle support, *J. Struct. Mech. Earthquake Eng.*, JSCE, No. 724(I-62), pp. 49–67, 2003. (in Japanese)
10) Cowper, G. R.: The shear coefficient in Timoshenko's beam theory, *J. Appl. Mech.*, ASME, Vol. 33, June, pp. 335–340, 1966.
11) Timoshenko, S. P.: On the correction for shear of the differential equation for transverse vibrations of prismatic bars, *Phil. Mag.*, Ser. 6, Vol. 41, pp. 744–746, 1921.

12) Wang, C. M., Reddy, J. N. and Lee, K. H.: *Shear Deformable Beams and Plates: Relationships with Classical Solutions*, Elsevier, 2000.

13) Elgaaly, M., Seshadri, A. and Hamilton, R. W.: Bending strength of steel beams with corrugated webs, *J. Struct. Eng.*, ASCE, Vol. 123, No. 6, pp. 772–782, 1997.

14) Yamaguchi, K., Yamaguchi, T. and Ikeda, S.: The mechanical behavior of composite prestressed concrete girders with corrugated steel webs, *Conc. Lib.*, JSCE, No. 31, pp. 183–210, 1998.

15) Dym, C. L. and Shames, I. H.: *Solid Mechanics: a Variational Approach*, McGraw-Hill, Inc., 1973.

16) Reddy, J. N.: *Energy and Variational Methods in Applied Mechanics: with an Introduction to the Finite Element Method*, John Wiley & Sons, 1984.

17) Research Group of Composite Structures with Corrugated Steel Webs: *Design manual of PC box girders with corrugated steel webs (Draft)*, Japan, Tokyo, 1998. (in Japanese)

18) Zienkiewicz, O. C. and Taylor, R. L.: *The Finite Element Method, 5th Edition*, Butterworth-Heinemann, 2000.

19) Tessler, A. and Dong, S. B.: On a hierarchy of conforming Timoshenko beam elements, *Comput. Struct.*, Vol. 14, No. 3–4, pp. 335–344, 1981.

20) Hughes, T. J. R., Taylor, R. L. and Kanoknukulchai, W.: A simple and efficient finite element for plate bending, *Int. J. Numer. Methods Eng.*, Vol. 11, pp. 1529–1543, 1977.

21) *ABAQUS: user's Manual, version. 6.3*, Hibbit, Karlsson & Sorenson, Inc., 2002. (CD-ROM)

22) Ata, Y., Ochiai, M., Mizoe, Y. and Machida, F.: A static and fatique test with full scale models for PC box girder bridge using corrugated steel webs, *J. Prest. Conc*, Japan, Vol. 43, No. 4, pp. 72–81, 2001. (in Japanese)

(Received October 7, 2003)